Scanning tunneling microscope assisted nanostructure formation: Two excitation mechanisms for precursor molecules

I. Lyubinetsky, S. Mezhenny, W. J. Choyke,[a] and J. T. Yates, Jr.[b]
Surface Science Center, Department of Chemistry, University of Pittsburgh, Pittsburgh, Pennsylvania 15260

(Received 21 May 1999; accepted for publication 23 July 1999)

The scanning tunneling microscope in a near-field emission mode has been employed to create nanostructures using the hexafluoroacetylacetonate Cu (I) vinyltrimethylsilane precursor molecule on the Si(111) surface at 300 K. Two distinctive mechanisms controlling the nanostructure formation have been delineated. The first process involves excitation of the molecule by the applied electric field, and the field induced surface diffusion acts to supply molecules to the nanostructure growth region under the tip. The second mechanism involves the dissociation of the molecule by an electron attachment process. The generated nanostructure topology is quite different for each excitation mechanism. Narrow cone-like structures are produced by the electric field while broad structures of lower height are produced by the electron attachment process. Both mechanisms operate simultaneously in the low bias voltage regime ($V<8$ V), with the field activated process dominating. The electron induced process becomes the governing process at higher voltages.
© *1999 American Institute of Physics.* [S0021-8979(99)02321-X]

I. INTRODUCTION

The use of the scanning probe microscope for the fabrication of structures down to the nanometer scale is of great current interest. Among these techniques, the scanning tunneling microscope (STM)-assisted local chemical vapor deposition (CVD) process has been employed to create nanostructures from a number of metals[1–6] and semiconductors.[7–11] These STM-assisted CVD studies were somewhat phenomenological and the optimal formation parameters in all studies, except Ref. 11, were determined on empirical grounds. Several mechanisms of nanostructure growth have been discussed, including the electron impact dissociation of a precursor molecule,[3–5,11] field-induced molecular dissociation,[3,5] and field-assisted molecular decomposition on the tip with subsequent field desorption of the fragments.[8] The exact mechanism has not been established, though in every case the operation of a single process has been implied.

The work reported here shows that two different mechanisms controlling nanostructure formation operate at positive sample bias voltage. The first excitation mechanism involves field-induced diffusion and decomposition of the precursor molecule under the tip. The second excitation mechanism causes the dissociation of the molecule by an electron attachment process. The two mechanisms result in quite different nanostructure topologies. Hexafluoroacetylacetonate Cu(I) vinyltrimethylsilane, [Cu^I (hfac) (vtms)], has been employed as a precursor molecule. This molecule is commonly used for conventional copper CVD.[12]

II. EXPERIMENT

The experiments were conducted in an ultrahigh vacuum (UHV) chamber (base pressure $\sim 6\times10^{-11}$ Torr) equipped with a STM (Omicron), an Auger electron spectrometer (Physical Electronics Industries), and a quadrupole mass spectrometer (UTI). Si(111) samples (*p* type, 150 Ω cm, Virginia Semiconductors) were degassed at ~900 K and subsequently cleaned by several 5 s flashes at 1500 K yielding the Si(111)-(7×7) reconstructed surface. STM tips were made from electrochemically etched tungsten wire. The tips were cleaned and sharpened *in situ* by annealing and Ar^+ bombardment, using the self-sputtering process in the field emission mode. The Cu^I (hfac) (vtms) precursor gas (Schumacher) was introduced through a stainless steel doser terminated with a 3 mm diameter orifice 4 cm away from the STM tunneling junction at an angle of 80° with respect to the surface normal. During nanostructure formation, a precursor flux of 2.6×10^{12} molecules/cm^2 s has been normally used. The nanostructure growth process has been carried out at 300 K during continuous dosing with the STM operating in a near-field emission regime (the sample bias voltage is positive and more than the work function). The tunneling current has been held constant with an active feedback loop. Before the nanostructure growth, the silicon surface has been dosed with Cu^I (hfac) (vtms) molecules up to the saturation coverage, which is in the submonolayer range on Si(111)-(7×7) at 300 K.[13]

III. RESULTS

Before the addition of the precursor gas to the surface, the experiments on surface modification have been carried out using the parameters to be used for growth (constant current of 0.01–1 nA at sample bias voltage, V, up to +45 V). Some increase of the defect number has been found, but, without additional exposure of the precursor, no growth of any features has been observed. Using the same parameters with simultaneous dosing by precursor, the formation of nanostructures has been accomplished.

[a]Also at Department of Physics and Astronomy, University of Pittsburgh, Pittsburgh, PA 15260.
[b]Electronic mail: jyates@vms.cis.pitt.edu

 © 1999 American Institute of Physics

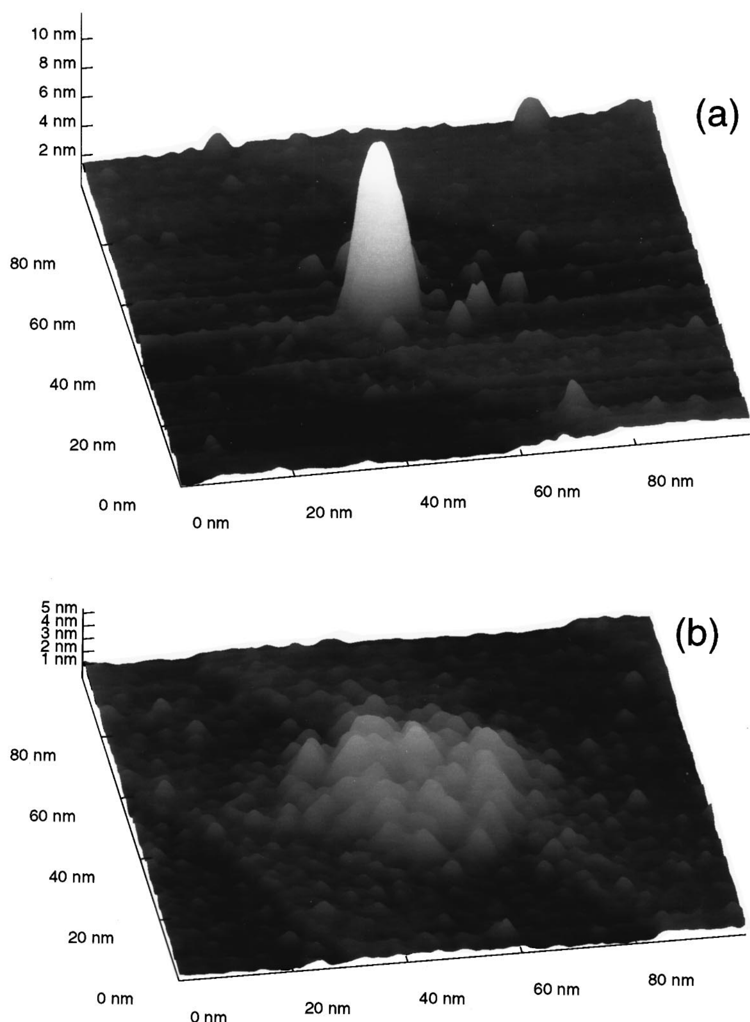

FIG. 1. Constant current images ($V=2$ V, $I=0.01$ nA) in 3D representation showing the typical topology of the nanostructures created: (a) at applied bias voltages, V, of 6 V and (b) at $V=11$ V. Other parameters were: $I=0.01$ nA, $F=2.6\times10^{12}$ molecules/cm^2 s, $t=5$ min.

We have observed strikingly different topologies of the nanostructures for different regimes of the applied bias voltage. At voltages less than 7 V, the created features exhibit relatively narrow cone-like structure with a high aspect ratio. In Fig. 1(a), a nanostructure created at $V=6$ V with a full width at half maximum, FWHM, of ~7.6 nm and a height of 10.5 nm is shown. Growth at higher voltages ($V>10$ V) leads to broad structures of lower height. The structure, shown in Fig. 1(b) for $V=11$ V, has an overall FWHM of 43 nm and a height of about 2 nm. Figure 2 presents the dependencies of the nanostructure volume as a function of the growth time for different bias voltages. For voltages more than 10 V, represented by the curve for $V=12.5$ V, the dependence is linear. At voltages less than 7 V (as shown for $V=5.5$ V), the curve starts linearly and then saturates, indicating that the growth process has stopped. In the intermediate voltage region, represented by curve for $V=7.5$ V, after some time the curve slope decreases but does not show saturation behavior. From the slope of the dependencies in the initial linear region, the growth rates have been determined for each regime.

The dependencies of the nanostructure growth rate on current for different voltage regimes are shown in Fig. 3. For growth at $V=12.5$ V, the curve starts from zero and is linearly dependent on current, which shows that this process is current induced. In the low voltage regime, the growth rate does not depend on current and, thus, the growth is apparently affected by another major factor, namely, by the electric field generated by the applied bias voltage. While Fig. 3 presents only initial parts of curves up to a current of 0.05 nA, the dependencies have been measured up to 0.3 nA (and have been found to continue linearly). In the intermediate voltage region, there is a linear dependence on current but

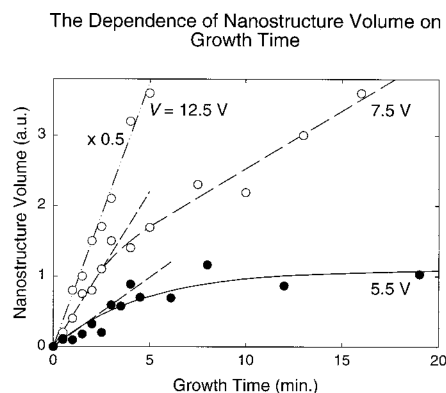

FIG. 2. Dependence of the nanostructure volume on exposure time for different regimes of bias voltages, and at $I=0.01$ nA. The slope of the dependency is proportional to the growth rate.

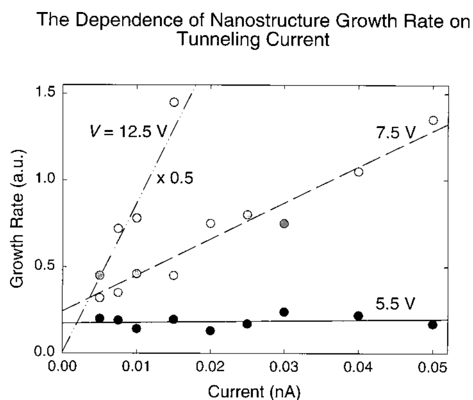

FIG. 3. Dependence of nanostructure growth rate on tunneling current for different regimes of bias voltages; the lines are linear regressions.

also the offset is present at zero current. We suggest that this behavior is caused by simultaneous operation of the two different processes, current and field induced, in the intermediate region. From such dependence on current, growth rates for both processes can be extracted, employing the fact that the offset corresponds to the growth rate for the field-induced process.

After separation of the rates of the current and field-induced processes in the voltage region where they overlap, the effect of the tip-sample bias voltage on growth rate for both mechanisms of nanostructure formation is demonstrated in Fig. 4(a). The current-induced process exhibits a threshold near 4.5 V bias, and the growth rate nearly saturates at voltages above 13 V. The field-induced process starts at $V>4$ V, shows a sharp maximum in rate near 6.5 V, and then decreases as the bias voltage increases further. The field-induced process has been also found to depend on the tip radius with the curve shifting to higher voltage for duller tips, while the current-induced dependence, as expected, is insensitive to the tip radius. Figure 4(b) shows the evolution of the nanostructure FWHM with bias voltage for both field- and current-induced processes. The FWHM of the field-induced nanostructures has been measured after the nanostructure dimensions have reached saturation maximum (see Fig. 2). The FWHM of the field-induced features is found to be approximately constant (~7 nm), while the FWHM of the current-induced features increases exponentially with bias up to the several 100 nm.

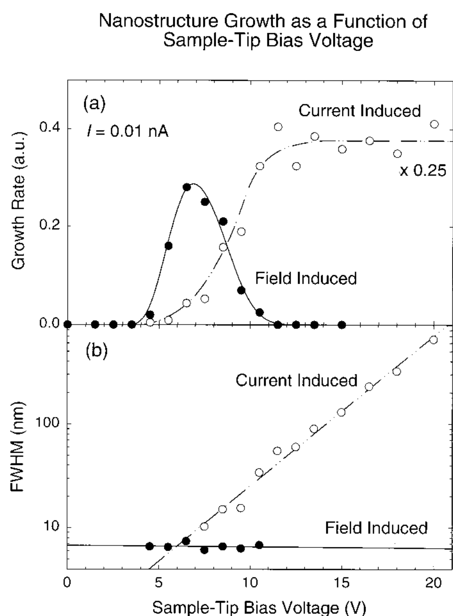

FIG. 4. Effect of the tip-sample bias voltage on (a) growth rate and (b) FWHM for field- and current-induced processes at $I=0.01$ nA. The FWHM of the current induced nanostructures at $V<8$ V cannot be determined directly because of overlap with the field activated process, which is much more efficient at these voltages, but it can be estimated from extrapolation (solid line).

IV. DISCUSSION

Both measured current and time dependencies (Figs. 2 and 3) have been found to be quite different at small (<7 V) and higher (>10 V) bias voltages, indicating that a different excitation mechanism, current and field induced, governs each regime, respectively. Evidently, as is shown from voltage dependencies, Fig. 4(a), the field-induced process determines nanostructure growth in the low bias voltage regime ($V<7$ V), the current-induced nanostructure formation dominates at voltages higher than 10 V, while both processes overlap in the intermediate voltage region.

The observed growth rate dependence on bias voltage for the current-induced process gives information relevant to the precursor molecule excitation mechanism. The direct ionization of the precursor molecule by electron impact can be excluded in the threshold regime, since the observed voltage threshold of ~4.5 V is too small to be caused by direct ionization. It is well known that an incident electron can be captured by an adsorbed molecule to form a temporary negative ion state,[14] which, if not quenched or desorbed, can decay through dissociation. The dissociation produces a surface fragment which can then be bound to the surface. This electron impact excitation mechanism is responsible for the current-induced nanostructure formation from the Cu^I (hfac) (vtms) precursor molecules. In separate experiment with a macroscopic electron beam on a Si(111) surface exposed to Cu^I (hfac) (vtms), a threshold electron energy of 4 eV was measured for dissociation by electron attachment.[15] Dissociative electron attachment (DEA) has also been suggested as deposition mechanism for the STM-induced decomposition of SiH_4 on Si(111).[11] The cross section for electron capture exhibits a maximum when the electron energy matches the energy of a lowest unoccupied molecular orbital. Although in the work reported here we did not observe a maximum in the growth rate dependence, its steep (two order of magnitude) increase at voltages above the threshold can be caused by overlap with several unoccupied states of the large Cu^I (hfac) (vtms) molecule.[16] With increasing voltage a direct ionization process can also contribute to the precursor dissociation. Additional support for the electron-induced excitation mechanism comes from observation that electron-induced growth does not occur at opposite bias polarity (sample bias is negative).[17] When the electrons are emitted from the tip at positive sample bias, V, they gain kinetic energy, eV, at the sample surface, causing excitation of ad-

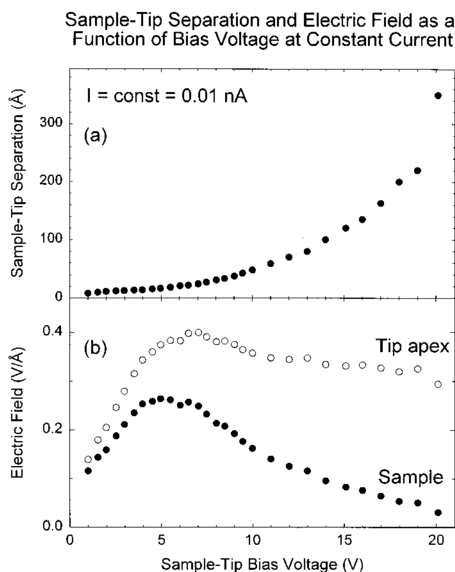

FIG. 5. (a) Tip-sample separation and (b) electric field on the sample and tip surface as a function of the tip-sample bias voltage at a constant current of 0.01 nA.

sorbed precursor molecules, while at opposite polarity electrons do not have sufficient energy at the surface to decompose precursor molecules.

To understand the observed evolution of the growth rate with bias voltage for the field-induced process [Fig. 4(a)], we have determined the dependence of the electric field at the sample and tip apex surfaces as a function of the applied voltage.[18] This has been accomplished by using the dependence of the tip-sample separation as a function of the bias voltage at constant current, shown in Fig. 5(a). To determine the ordinate for Fig. 5(a), the tunneling gap has been calibrated from contact point measurements using the tunneling current dependence on the tip-sample separation.[19] For small bias voltages (in the tunneling regime), the separation changes almost linearly with applied voltage. At higher voltages (in the field emission regime), the separation deviates from linear behavior exhibiting an exponential increase, with a higher rate of change for sharper tips.[20] Comparison of this curve with the voltage dependence of the nanostructure FWHM [Fig. 4(b)] demonstrates that the width of the current-induced nanostructure is primarily affected by the tip-sample separation, which determines the distribution of electron flux emitted from the tip.[21]

We have calculated the field at the sample surface, F_S, and at the tip apex, F_T, using the expression obtained by solving the Laplace equation within an analytical approximation,[22]

$$F_S=\frac{2V}{S^{1/2}(S+R)^{1/2}}\left\{\ln\left[\frac{(S+R)^{1/2}+S^{1/2}}{(S+R)^{1/2}-S^{1/2}}\right]\right\}^{-1}, \quad (1)$$

$$E_T=\frac{2V(S+R)^{1/2}}{RS^{1/2}}\left\{\ln\left[\frac{(S+R)^{1/2}+S^{1/2}}{(S+R)^{1/2}-S^{1/2}}\right]\right\}^{-1}, \quad (2)$$

where S is the tip-sample separation, and R is the tip radius. In the calculations, we have used a 5 nm tip radius, estimated from the measured field emission characteristics of the tip.[22,23] Figure 5(b) shows the dependence of the electric field on tip and sample surfaces as a function of the bias voltage. There is a qualitative change in the field evolution on the tip surface after the transition from the tunneling to the field emission regime. In the tunneling regime, the field increases almost linearly. In the field emission regime, the field is almost constant at the tip surface. A constant current mode in the field emission regime implies an approximately constant field at the emitter (negative biased) surface, as has been measured. This constant field behavior obviously cannot explain the observed dependence of the growth rate on bias voltage [Fig. 4(a)] and, therefore, indicates that a field-induced deposition process on the tip is improbable.

The curve for the electric field on the sample surface has an asymmetric peak-like shape with a maximum close to 0.27 V/Å at a bias voltage around 5 V, and then decays at higher bias voltage. Comparison of this curve with the voltage dependence of the growth rate for the field-induced process [Fig. 4(a)] shows their similarity and indicates that the *electric field on the sample surface* is the main factor that controls this process. One can also see by comparison Fig. 4(a) to Fig. 5(b), that the field-induced nanostructure growth begins to take place when the field exceeds some critical level of ~0.2 V/Å. The observed termination of the growth at positive bias voltages more than 11 V may be partially understood as due to the decrease of the field to less than the critical level in this region, which halts the precursor dissociation.

Our data also indicate that the field-induced surface diffusion of the precursor species plays an important role in the nanostructure formation. We have found (from the nanostructure size dependence upon the exposure time, Fig. 2) that as the formation goes on, there is a significant decrease of the growth rate of nanostructures compared to the initial stages of growth for the field-induced process. This may be caused by the reduction of the field-induced diffusion of precursor species from the outer surface region to the region under the tip as the nanostructure grows higher (and the tip is moved farther from the sample surface by feedback). The diffusion is induced by the electric field gradient which arises from the proximity of the STM tip to the sample surface.[24] It has been also found that the rate of nanostructure growth exceeds (approximately by one to two orders of magnitude) the rate of delivery of precursor molecules to the region directly under the tip. This is another indication that field enhanced surface diffusion plays a role in the nanostructure formation process.[5] Since chemisorption of the precursor molecules does not occur above the first monolayer and, indeed, the first layer chemisorbed molecules do not diffuse at room temperature,[18] the molecules apparently physisorb in a second layer and diffuse under the action of the field during their adsorption life time. Hence, the field-induced process involves field-induced surface diffusion of the precursor molecules as was discussed above, their activation by the electric field, and the accumulation of decomposed material underneath the tip.

V. CONCLUSION

In summary the following features of STM-induced nanostructure growth have been found:

(1) Excitation of the precursor molecule, Cu^I (hfac) (vtms), occurs as a result of the applied electric field. Field strengths above ~0.2 V/Å are required.
(2) Narrow cone-like nanostructures are produced by the field-induced growth mechanism.
(3) Excitation of the precursor also occurs as a result of electron attachment to the molecule. The threshold electron energy for this process is about 4.5 eV.
(4) The electron attachment mechanism produces flat and broad nanostructures.
(5) Both of these mechanisms act together in the low bias voltage regime ($V < 8$ V).

ACKNOWLEDGMENT

The authors thank the Army Research Office for the support of this work.

[1] E. E. Ehrichs, R. M. Silver, and A. L. de Lozanne, J. Vac. Sci. Technol. A **6**, 540 (1988); S. Rubel, M. Trochet, E. E. Ehrichs, W. F. Smith, and A. L. de Lozanne, *ibid*. **12**, 1894 (1994).
[2] M. A. McCord, D. P. Kern, and T. H. P. Chang, J. Vac. Sci. Technol. B **6**, 1877 (1988).
[3] A. D. Kent, T. M. Shaw, S. von Molnar, and D. D. Awschalom, Science **262**, 1249 (1993).
[4] D. S. Saulys, A. Ermakov, E. L. Garfunkel, and P. A. Dowben, J. Appl. Phys. **76**, 7639 (1994).
[5] A. Laracuente, M. J. Bronikowski, and A. Gallagher, Appl. Surf. Sci. **107**, 11 (1996).
[6] W. W. Pai, J. Zhang, J. F. Wendelken, and R. J. Warmack, J. Vac. Sci. Technol. B **15**, 785 (1997).
[7] G. Dujardin, R. E. Walkup, and Ph. Avouris, Science **255**, 1232 (1992).
[8] T. M. H. Wong, S. J. O'Shea, A. W. McKinnon, and M. E. Welland, Appl. Phys. Lett. **67**, 786 (1995).
[9] H. Rauscher, U. Memmert, and R. J. Behm, J. Vac. Sci. Technol. B **13**, 1217 (1995).
[10] D. Samara, J. P. Williamson, C. K. Shih, and S. K. Banerjee, J. Vac. Sci. Technol. B **14**, 1344 (1996).
[11] H. Rauscher, F. Behrendt, and R. J. Behm, J. Vac. Sci. Technol. B **15**, 1373 (1997).
[12] P. Doppelt and T. H. Baum, MRS Bull. **19**, 41 (1994), and references therein.
[13] I. Lyubinetsky, S. Mezhenny, W. J. Choyke, and J. T. Yates, Jr. (unpublished).
[14] L. Sanche, Scanning Microsc. **9**, 619 (1995).
[15] S. Mezhenny, I. Lyubinetsky, W. J. Choyke, and J. T. Yates, Jr., J. Appl. Phys. **85**, 3368 (1999).
[16] Unfortunately, to the best of our knowledge, information on the low energy electron-induced resonance excitation of the Cu^I (hfac) (vtms) molecules is not available in the literature.
[17] I. Lyubinetsky, S. Mezhenny, W. J. Choyke, and J. T. Yates, Jr., J. Vac. Sci. Technol. A **17**, 1445 (1999).
[18] The calculated electric field has been used for evaluation of the field-induced process only at initial growth stages, where the surface is not far from flat.
[19] J. K. Gimzewski and R. Möller, Phys. Rev. B **36**, 1284 (1987); Y. Kuk and P. J. Silverman, J. Vac. Sci. Technol. A **8**, 289 (1990).
[20] J. J. Saenz and R. Garcia, Appl. Phys. Lett. **65**, 3022 (1994).
[21] T. M. Mayer, D. P. Adams, and B. M. Marder, J. Vac. Sci. Technol. B **14**, 2438 (1996).
[22] G. Mesa, E. Dobado-Fuentes, and J. J. Saenz, J. Appl. Phys. **79**, 39 (1996).
[23] R. Gomer, *Field Emission and Field Ionization* (American Vacuum Society Classics, AIP, New York, 1993).
[24] L. J. Whitman, J. A. Stroscio, R. A. Dragoset, and R. J. Celotta, Science **251**, 1206 (1991).